JARQ 56 (2), 147-161 (2022) https://www.jircas.go.jp

Design and Performance Analysis of a Seasonal Ice Storage System for Cooling Chinese Solar Greenhouses

Xuan GU[1], Rui WANG[1,2], Tianlai LI[1] and Hui XU[1]*

[1] Horticultural College, Shenyang Agricultural University, National and Local Joint Engineering Research Center of Northern Horticultural Facilities Design and Application Technology, Shenyang, China

[2] Institute of Vegetable and Floriculture Science, National Agriculture and Food Research Organization, Tsukuba, Japan

Abstract

To identify an energy-saving solution to cool Chinese solar greenhouses during summer nights, we present a design for a seasonal ice storage system that uses a storage tank to store winter cold energy in water to serve as a source of cold air in the summer. The parameters of the seasonal ice storage system were designed based on the cooling demand of the greenhouse in the summer. To optimize the cooling effect in the heat exchange system, a computational fluid dynamics model was developed to select the size of the heat transfer pipes, and a validation experiment was conducted in the greenhouse. The impacts of the insulation material and size of the heat exchange pipes on system performance have been discussed. The field experiment was conducted in Shenyang to validate the performance of the ice storage system. The best cooling effect in cultivation area was 6.7°C, and the average temperature difference between the beginning and end of the run in the greenhouse was 4.4°C. This system increased heat exchange performance while lowering air temperature in the greenhouse.

Discipline: Agricultural Engineering

Additional key words: computational fluid dynamics, optimize, temperature, winter

Introduction

Solar greenhouses have realized the cultivation of crops at −20°C in winter in northeast China because of the heat storage structure; however, because the heat storage structure stores too much heat during the day in summer, the temperature in the greenhouse at night is too high, affecting the quality and yield of crops (Álvarez-Prado & Ploschuk 2008, Ghani et al. 2019, Kim 2007, Kumar et al. 2009, Pakari & Ghani 2019, Verheul et al. 2007). At the same time, the temperature difference between day and night not only affects the morphological characteristics of crops, such as internode length (Davies et al. 2002) and plant height (Blanchard & Runkle 2011, Patil & Moe 2009), but also significantly affects crop growth and fruit yield and quality (Chen et al. 2014, Fleisher et al. 2006) by affecting material accumulation and distribution (Hwang et al. 2005, Mao et al. 2012, Yang et al. 2014) and flower bud differentiation (Catley et al. 2002, Erwin et al. 2002, Warner & Erwin 2001). Therefore, considering crop production, it is important to cool Chinese solar greenhouses at nighttime during summer.

At present, the main cold resources for greenhouses are water and soil. Evaporative cooling is often used in greenhouses, with water as cold resources (López et al. 2012, Perdigones et al. 2008). Additionally, the heat exchange system uses water and soil as cold resources. The geothermal heat pump system uses surface soil or groundwater as a cold or heat source to drive the circulation through the pump, which runs all year round. In winter, the underground soil or water source heat is sent to the greenhouse through a heat pump for warming in the solar greenhouse. In summer, the excess heat in the room is transferred to the soil or water for cooling in the solar greenhouse. Although the system has high energy-saving efficiency, its initial investment is large, and construction is inconvenient (Cui et al. 2019, Sellami et al. 2019). A water source heat pump uses shallow water source on the surface of the earth to form low-grade thermal energy resources, such as solar energy and geothermal energy absorbed in groundwater, rivers,

*Corresponding author: xuhuiaa@126.com

Received 1 October 2020; accepted 28 April 2021.

and lakes. This new technology is more energy efficient, environmentally friendly, and convenient than a geothermal heat pump; however, it is only applicable for water-rich areas (Ni et al. 2007, Sun et al. 2017). The earth–air heat exchange system (Bordoloi et al. 2018, Ozgener & Ozgener 2010, Yıldız et al. 2012) uses indoor air and surface soil temperature difference for the heat exchange to cool. The underground aquifer–air heat exchange system (Sethi & Sharma 2007) uses the underground aquifer or surface water as cold source to exchange heat with the indoor hot air. Compared with the heat pump technology, this system cooling principle is directly conducted through the temperature difference between the cold source and indoor air without the heat pump unit. However, although this technology has a low initial cost and simple construction, the temperature difference between the greenhouse air at night in summer and the surface soil or water storage layer is small, the heat transfer performance is reduced, and the cooling capacity is insufficient. On one hand, the temperature of the water and soil is relatively high, which cannot meet the demand of forced cooling at night in solar greenhouses during summer. On the other hand, the ice temperature is low; however, it has not been applied in greenhouse cooling.

The seasonal cold storage technology aims to store the natural cold energy of winter for the summer, realizing energy conservation and promoting environmental improvement (Yu et al. 2005). The cooling sources of the seasonal cold storage can be natural ice and snow, artificial snow and ice produced by cold ambient air, or frozen soil and rocks in winter. The first seasonal ice storage tank air conditioning system was built in 1979 at Princeton University. In winter, a part of the water is extracted from the ice storage tank; it is then made into snow by a snow making machine (Kirkpatrick et al. 1985). In Canada, Vigneault et al. (1990) used an abandoned storage space to build a wooden ice storage pool for vegetable preservation. This system consists of an ice making system and a vegetable precooling system. In the 1990s, the Illinois State University established a seasonal snow storage air conditioning system in an underground parking garage. The system was filled with a specified amount of gravel and water in an underground ice storage container, and the coils were precisely arranged in the container (Francis & Tamblyn 1987). In Japan, Hamada et al. established a hybrid snow storage and melting air conditioning cold source system that combined an air cooling system and a water loop cooling system for cooling in a building (Hamada et al. 2007, 2012). In Sweden, Sundsvall Hospital used a water loop cooling system for seasonal snow storage cooling studies. The system used the heat exchange between water and snow to complete the extraction and distribution of the cold. In the summer, the water that melted at the bottom of the snow storage tank was cooled by the heat exchanger to the air conditioning system; then, the circulating water was returned (Skogsberg 2002).

In northern China, remarkable results have been achieved (Li et al. 2003). For example, based on the actual situation of air conditioning cooling in the cold regions of northern China, Liu and Guan (2009) built a snow storage pool near the airport cooling station for cooling the building during summer. Yu et al. (2010) established a heat transfer mathematical model for a cylindrical underground storage based on the steady-state heat transfer and lumped-parameter method for four typical buildings in Beijing. Additionally, Li et al. (2015) established the mathematical model for the unsteady heat transfer in an underground cylindrical ice storage to undertake the central air conditioning project of a gymnasium in Harbin and Shijiazhuang. Yan et al. (2016a) described a system with a storage volume of 450 m^3 that could provide about one-third of the total cooling demand of a building with a total gross area of 2,000 m^2. Yan et al. (2016b) also studied a compound system with a storage volume of 351 m^3 that could provide sufficient cooling for a 2,000 m^2 building in Beijing. Numerous studies have shown that, as a renewable natural cold source, seasonal ice storage technology has the advantages of being effective, economic, and environmentally friendly and having reduced noise, and most projects are cost effective.

Although seasonal cold storage systems have been used in some residential applications, it has not yet been reported in solar greenhouses. Most solar greenhouses in China are built in cold regions, where the natural cold resource is abundant. Therefore, an investigation on the use of seasonal ice storage for cooling solar greenhouses is potentially of great value. Existing studies have validated the use of this method; however, there remains no systematic exploration of the implications of using this type of cooling system in a greenhouse. To fill this gap, our study introduces the design of an ice–air heat exchange system that uses ice as cold source for Chinese energy-saving solar greenhouses (CESG) to reduce the temperature during summer nights based on the phenological conditions suitable for cold storage in northeastern China. The parameters of the seasonal ice storage system have been calculated, and the heat exchange of the pipes in the ice storage tank was also calculated using a computational fluid dynamics (CFD) model for characterizing the dynamic process. The simulated and monitored data were analyzed based on a field application in Shenyang to demonstrate the effective performance of the proposed system. This system solves the problem of high temperature at night for Chinese solar greenhouses during summer.

Design of the seasonal ice storage system

A schematic diagram of the seasonal ice storage cooling system used for solar greenhouses is shown in Figure 1. The system consists of two parts: the ice storage heat exchanger and the ice storage tank. The ice storage heat exchanger tank is located outside the greenhouse, using a stratified, open underground storage method. In winter, the outdoor cold energy is used to freeze the water in the ice storage tank to store the cooling energy used for cooling in summer. In the summer, indoor hot air is circulated with a fan to the heat exchanger in the ice storage tank, and the cooled air is sent back to the greenhouse.

Methodology

1. Calculation of parameters for the seasonal ice storage system

The total cold storage capacity of the ice storage tank should satisfy the total cooling capacity of the stored ice, which is greater than or equal to the cooling capacity required for summer cooling and the cooling loss during storage. According to formula 2.3 in Li (2015), the ice storage volume was calculated as follows (Eq. 1):

$$V_{\mathrm{i}} = (Q_{\mathrm{cool}} + Q_{\mathrm{loss}}) \,/\, [\rho_{\mathrm{ic}}c_{\mathrm{ic}}(0 - T_0) + \rho_{\mathrm{ic}}h_{\mathrm{fg}} + \rho_{\mathrm{wa}}c_{\mathrm{wa}}(T_{\mathrm{lim}} - 0)] \tag{1}$$

According to the air energy calculation formula (formula 2.4) in Ou (2015), where $Q_{\mathrm{cool}}=Q_{\mathrm{f}}+Q_{\mathrm{c}}$, Q_{f} was calculated as follows (Eq. 2):

$$Q_{\mathrm{f}} = c_{\mathrm{a}}\rho_{\mathrm{a}}V_{\mathrm{G}}(T_{\mathrm{b-ind}} - T_{\mathrm{ind}})D \tag{2}$$

According to Yang and Tao (2006) in Chapter 1 of Heat Transfer (pages 4-15), Q_{c} was calculated as follows (Eq. 3):

$$Q_c = \sum A_{\mathrm{Ge}}K_{\mathrm{Ge}}(T_{\mathrm{outd}} - T_{\mathrm{ind}}) + \sum A_{\mathrm{s}}h_{\mathrm{s}}(T_{\mathrm{s}} - T_{\mathrm{ind}}) + \sum c_{\mathrm{a}}\rho_{\mathrm{a}}V_{\mathrm{G}}\mathrm{n}(T_{\mathrm{outd}} - T_{\mathrm{ind}}) \tag{3}$$

where h_{s} is obtained using the empirical formula $Nu=0.27(GrPr)^{1/4}$, $h_{\mathrm{s}}=NuL_{\mathrm{s}}/\lambda$. The parameter values were substituted into the equation to obtain the total energy from June to August: $Q_{\mathrm{cool}} = 1.75 \times 10^{10}$ J.

Q_{loss} was calculated using Eq. 4:

$$Q_{loss} = \sum A_{\mathrm{n}}K_{\mathrm{n}}\Delta t_{loss} \tag{4}$$

where $K_{\mathrm{n}} = 1 \,/ \sum(\delta_{\mathrm{n}} \,/\, \lambda_{\mathrm{n}})$. In this study, we only considered the thermal resistance of brick walls and insulation materials. δ_{b} was the conventional construction standard of 0.24 m.

To reduce the external surface area of the ice storage tank, its shape was designed as an equilateral long cube. In the winter of Shenyang from December to February, the maximum accumulated freezing index was 24 Kh, and the minimum accumulated freezing index was 18.5 Kh (Kusakabe 1962). The frozen soil layer in Shenyang was 1.5-m deep, and the lowest temperature that could be reached was –20 °C K. It was difficult to dig below 2 m; therefore, we changed the depth of the ice storage tank to 2 m. In Eq. 1, it is shown that the thicker the thermal insulation material, the smaller the heat loss and smaller the ice storage tank volume. Therefore, the thickness of the thermal insulation material and the size of the ice storage pool determined the total cost.

The heat loss rate was calculated using Eq. 5, according to equations 2.1-2.10 of Li (2015) (pages 19-20):

$$1 - \omega = Q_{\mathrm{cool}} \,/\, 2b^2 \,/\, [\rho_{\mathrm{ic}}c_{\mathrm{ic}}(0 - t_0) + \rho_{\mathrm{ic}}h_{\mathrm{fg}} + \rho_{\mathrm{ic}}c_{\mathrm{wa}}(T_{\mathrm{lim}} - 0)] = 25.47 \,/\, b^2 \tag{5}$$

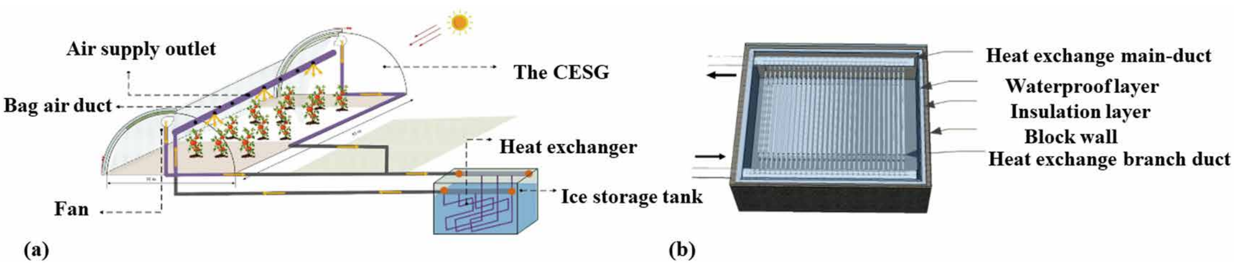

Fig. 1. Schematic diagram of the seasonal ice storage system
(a) Principle of cooling; (b) ice storage tank detail

The heat loss rate increases with the length of the ice storage tank, approaching 100%. The expanded polystyrene board was selected as the insulation material. As the thickness of the insulation material increases, the volume of the required ice storage tank decreases and becomes closer to the effective ice storage volume of Q_{cool}.

2. Heat transfer model

To optimize the cooling effect in the heat exchange system, a CFD model was developed using COMSOL Multiphysics to select the size of the heat transfer pipes and the validation experiment. Based on the actual heat storage structure of the ice storage tank, the calculation was large, requiring a long calculation time. The internal heat exchange tubes were arranged side by side, and each shape was of the same size; the difference between each inlet speed was small. For the convenience of calculation, two heat exchanger branches were selected for the modeling analysis. The geometric model parameters are shown in Figure 2. The heat exchange tube had a length of 16.2 m and a tube diameter of 0.05 m. The distance between the two tubes was 0.18 m. The tube was 0.5 m from the side wall of the ice storage tank and 0.4 m from the bottom.

3. Physical model simplification and boundary condition settings

According to the calculated size of the ice storage pond, we observed the changes in the internal conditions of the ice storage from winter to summer. It was found that there was still a lot of ice in the pool during summer, and the temperature in the pool was below zero. The physical model was simplified based on the above information.

The temperature of the ice was maintained at 0°C during the calculation.

The influence of water vapor condensation in the heat exchange pipe on the temperature and flow field was ignored.

Heat exchange varied in the different tubes, but at a short distance, it was considered equal.

The boundary condition parameters are shown in Table 1.

Table 1. Boundary condition parameters

Boundary condition	Parameters
Inlet temperature (°C)	30
Inlet speed (m/s)	14.3
Ice density (kg/m^3)	900
Specific heat capacity (J/ kg·k)	2.1×10^3
Thermal Conductivity (W/ m·k)	2.2

4. Mathematical model

Generally, the flow with a Reynolds number of less than 2,300 is laminar; Reynolds number of 2,300-4,000 indicates the transition state; and Reynolds number of greater than 4,000 is turbulent. This is calculated using

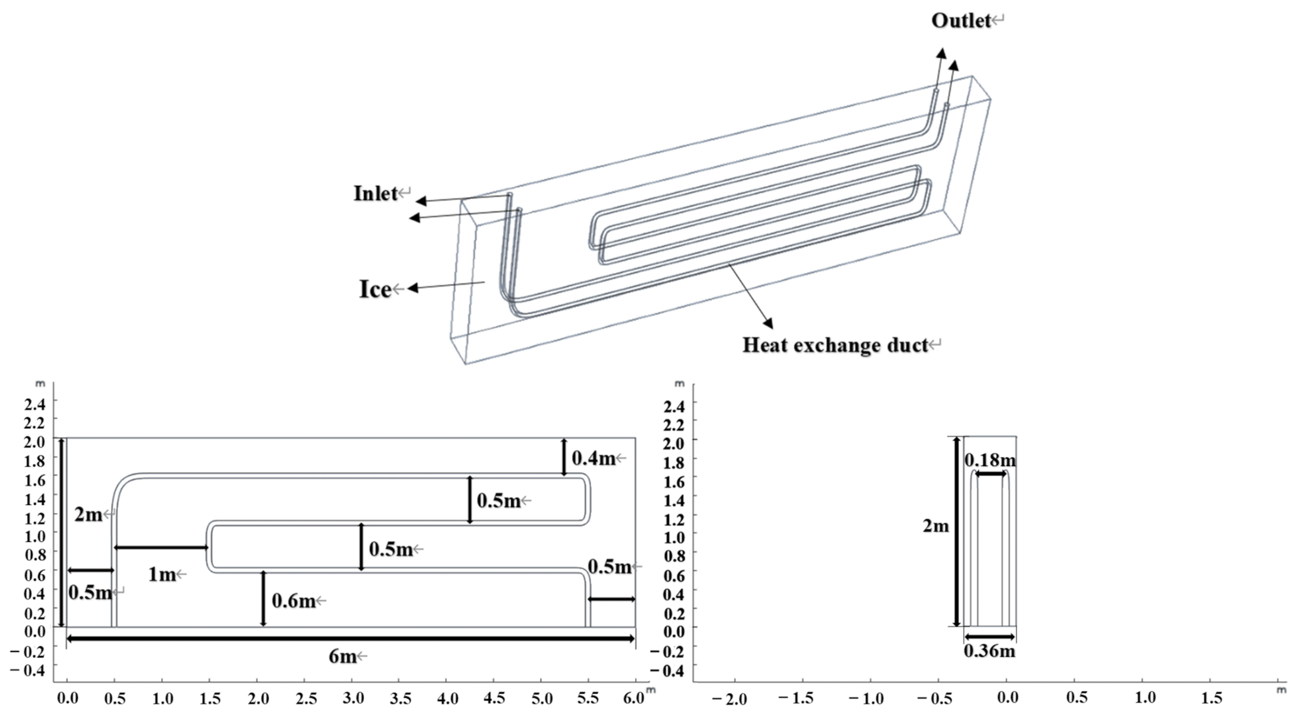

Fig. 2. Geometric model

the following formula from Yang and Tao (2006) in Chapter 6 of Heat Transfer (pages 250-252): $Re = \rho vL / \mu$. This paper designed the number of heat transfer tubes mainly based on the CFD model. The fluid condition in the tube was not specifically analyzed, and a laminar flow model was selected to save calculation time.

5. Heat exchange pipe length calculations

The main factors affecting the heat exchange efficiency (η) and the cost of the heat exchange structure were the length, number, and diameter of the tubes, as well as the material from which they were made. The relationship between the tube length and other parameters were calculated as follows (Eq. 6) (Wang et al. 2007):

$$\Phi = \rho_{\mathrm{a}} q_{\mathrm{v}} c_{\mathrm{a}} \triangle t_{\mathrm{tw}} = k_{\mathrm{tu}} L_{\mathrm{tu}} (t_{\mathrm{in}} - t_{\mathrm{out}}) \tag{6}$$

Ignoring the thermal resistance of the melting water layer, k was calculated using Eq.7:

$$k = \pi / [1 / hD_1 + ln(D_2 D_1{}^{1}) / 2\lambda_{\mathrm{tu}}] \tag{7}$$

h was calculated using Eq. 8:

$$h = Nu\lambda_{\mathrm{a}} / D_1 \tag{8}$$

When the fluid was cooled, the forced convection heat transfer in the tube was calculated as follows (Eq. 9):

$$Nu = 0.023Re^{0.8}Pr^{0.3} \tag{9}$$

where $Re=uD_1 / v$

Based on Eq. 6-9, the pipe lengths were determined using Eq. 10:

$$L = \rho q_{\mathrm{v}} c_{\mathrm{a}}\, ln(t_{\mathrm{in}} t_{\mathrm{out}}^{-1})[h^{-1} D_1^{-1} + ln(D_2 D_1^{-1}) / 2\lambda] / \pi \tag{10}$$

The greenhouse cooling supply air rate was calculated as follows (Eq. 11):

$$G = q_{\mathrm{c}} / (h_{\mathrm{N}} - h_{\mathrm{L}}) \tag{11}$$

where h_N and h_L were found in the humidity enthalpy chart (Li 2007).

Finally, we chose a centrifugal fan with a fan power of 2.5 KW.

6. System performance

System performance was mainly analyzed using η, Q_h, and coefficient of performance (COP), where $\eta=(t_{in}-t_{out} / t_{in}-t_{ic})$, $Q_h=c_a m_a(t_{in}-t_{out})$, and $COP=Q_h / E$, according to Mongkon et al. (2014) (Eq. 17-22).

Experimental validation of the model

1. The greenhouse

The test greenhouse (Fig. 3(a)) is a CESG located at the experimental station of Shenyang Agricultural University; the greenhouse is usually used to cultivate tomatoes in summer. Figure 3(b) shows the structural diagram of the greenhouse. The thermal cover of the greenhouse is composed of an insulating layer that can be moved at night in winter to maintain the thermal resistance of the greenhouse and opened in the day to receive energy from the sun. During the day, the side top vents can be used to take advantage of the natural ventilation of the greenhouse. To use the seasonal ice storage cooling system and reach the cooling temperature at night, the greenhouse was enclosed, and the thermal cover was closed at night. The test greenhouse's main structural parameters are given in Table 2.

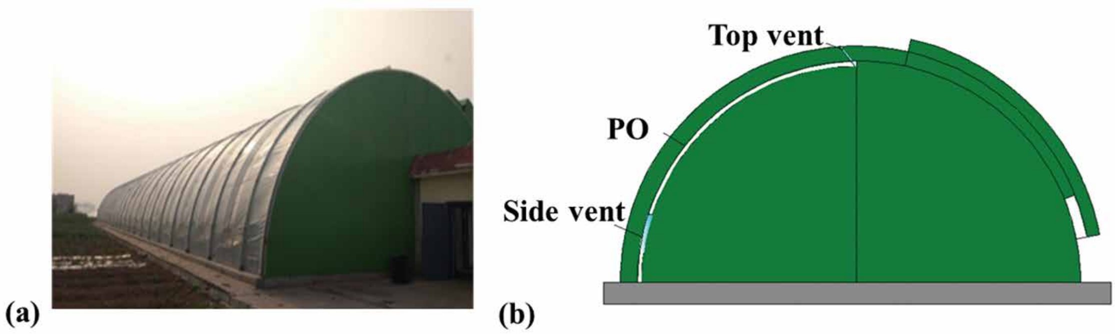

Fig. 3. The experimental greenhouse

(a) Photograph of the greenhouse; (b) greenhouse structural diagram

Table 2. Test greenhouse parameters

Width (m)	10
Length (m)	55
Height (m)	5
Area (m^2)	550
Greenhouse volume (m^3)	2,158.8
Roof lighting angle (°)	41.5
Enclosure thickness (m)	0.25
Enclosure thermal resistance (rock wool color steel plate) (m^2·K/W)	5.2

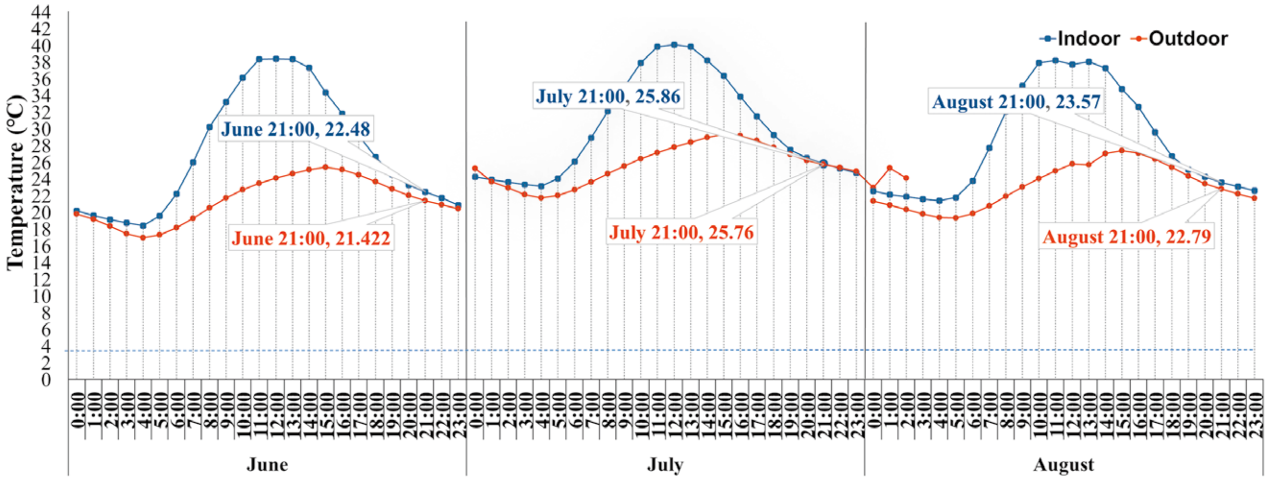

Fig. 4. Outdoor and indoor temperatures for the experimental greenhouse without cooling in June, July, and August of 2017

2. Basic principle behind the seasonal ice storage cooling system

Figure 4 shows the indoor and outdoor hourly temperatures for the test greenhouse without cooling during the summer in Shenyang. It is shown that the difference between the indoor and outdoor temperature is small at night and that the indoor temperature remains higher than the greenhouse design standard of 17°C (Li 2014). To meet the indoor maximum temperature cooling demand, the highest environmental parameters in July were used as the design reference.

3. Experimental details

The proposed seasonal ice storage system was applied to the CESG in Shenyang, and the heat exchange tubes are shown in Figure 5(a). The key parameters of the seasonal ice storage system are presented in Table 3 to validate the CFD model for the simulation of the heat exchange characteristics in the heat exchange tubes and obtain the optimum inlet and outlet temperatures, and a field experiment was performed as shown in Figure 5(b).

The test was designed as a simulation using two heat exchange tubes in the complete system to validate the CFD model. The measured fan exit speed was 28.5 m/s, and the fan outlet pipe diameter was 0.05 m. Ignoring the flow loss due to wall friction, the inlet speed of the branch was 14.25 m/s. On February 13, 2017, a plastic pipe was used to connect the heat exchange tube and greenhouse with the working high-pressure fan. The plastic pipe had better thermal insulation, and the thermal conductivity was 0.65 W/m·K. The distance between the heat exchange tubes and the greenhouse was 2 m. The T-type thermocouple wire of the CR-3000 data collector was placed in the inlet and outlet ends of the heat exchange tube and inside the ice tank to record the temperature data.

Table 3. Key parameters of the seasonal ice storage system

Parameters	Values	Parameters	Values	Parameters	Values
c_a	1,005 J/kg·°C	T_{lim} (Fang 2006)	10°C	T_{ind}	17°C
c_{ic}	2,100 J/kg·°C	T_0	0°C	T_{outd}	21.6°C
c_{wa}	4,200 J/kg·°C	$T_{b\text{-}ind}$ (Ghosal & Tiwari 2006)	26°C	T_s	26°C
ρ_a	1.29 kg/m^3	A_{Ge}	942 m^2	$\Delta t_{u\text{-}loss}$ (Li 2015)	8.5°C
ρ_{ic}	900 kg/m^3	A_s	550 m^2	$\Delta t_{t\text{-}loss}$	19.5°C
ρ_{wa}	1,000 kg/m^3	n (Zhang et al. 2013)	0.6 h	λ_b	1 W/m·K
h_{fg}	33,500 J/kg	h_s	0.49 W/m^2·K	λ_{eps}	0.041W/m·K
k_{Ge}	0.19 W/m^2·K	D	92 d		

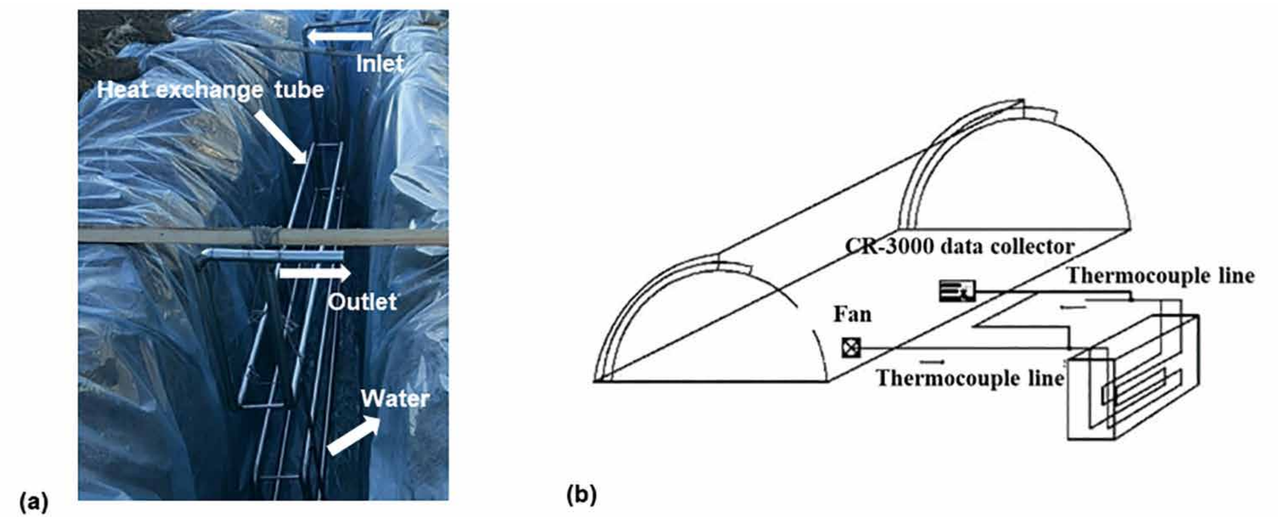

Fig. 5. Experimental apparatus and materials
(a) Implementation of the heat exchange system; (b) diagram showing the design of the experimental cooling system

4. Model verifications

Figures 6(a) and 6(b) show the measured tube inlet and outlet temperatures and temperature changes in the tank during the test. The inlet temperature was controlled at 30°C, and the outlet temperature was controlled at 2°C. Figure 6(c) is a curved-surface diagram showing the simulation results of the internal temperature change in the heat exchange tube, using the same inlet temperatures and speeds that were tested. The test measured an outlet temperature of 2.1°C and a simulation result of 1.6°C, and an outlet velocity of 13.9 m/s and a simulation result of 15.3 m/s. The temperature in the tank was measured as 0.8°C, and the simulated layer showed that the temperature in the tank was about 0°C. The simulation results show the same tendencies as the test results, and the values are similar.

5. Cooling effect verification test

The test was conducted at 11:00 on February 15, 2017. At 12:25, we closed the greenhouse to simulate the environment of a summer night and then started the fan at 13:12 to run the system. The cooling effect of each measuring point was recorded using CR-3000. The test placement photos and measuring point layout are shown in Figure 7.

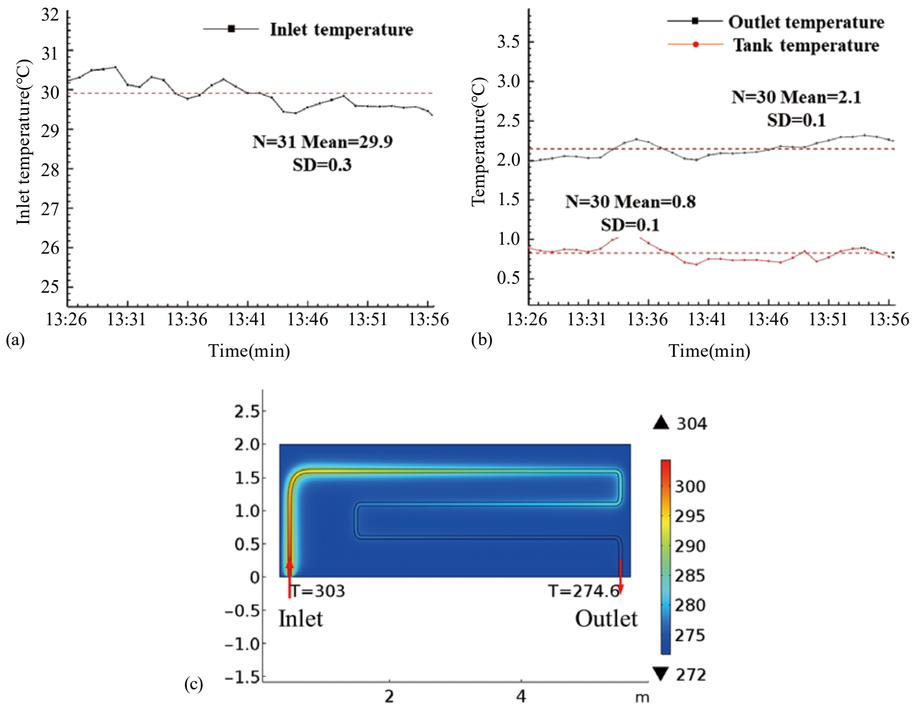

Fig. 6. Model verification

(a) Tube inlet temperature; (b) outlet and tank temperatures; (c) computational fluid dynamics (CFD) simulation results. Inlet T = 303 K, V = 14.25 m/s

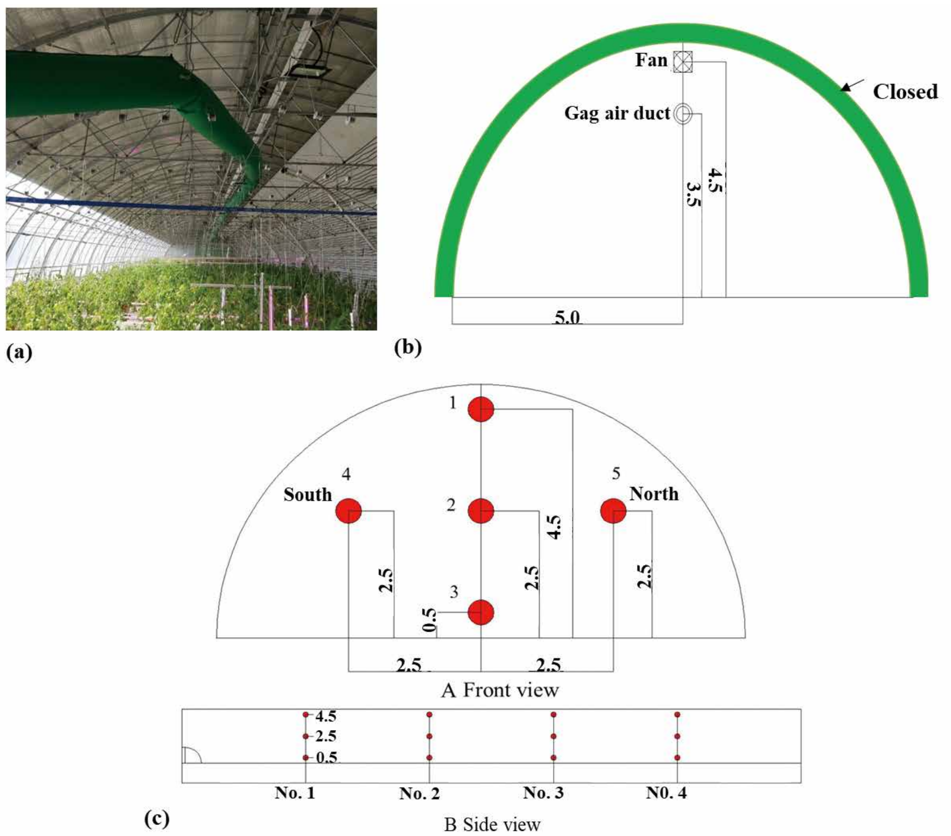

Fig. 7. Cooling test equipment

(a) Test photo; (b) equipment placement diagram (unit: m); (c) greenhouse measuring point layout (unit: m)

Results and discussion

1. Impact of the type of insulation material

To obtain the optimal tank volume for the actual construction, the thermal characteristics and cost of the insulation materials were considered. The total cost of the tank was determined by the block wall and insulation layer. As shown in Table 4, two insulation materials commonly used in ice storage tanks were selected. From the cost calculation, based on the thickness of the insulation material, heat loss from the ice storage tank decreased with increasing thickness of the insulation material, but the cost of construction was increased. When the thickness of the insulation layer was between 0.07 m and 0.1 m, the relative variation in heat loss tended to stabilize, and the cost of the ice storage tank was $2689, which is good in terms of price/performance ratio (Fig. 8).

2. Impact of the tube outlet temperature

The number and lengths of the tubes in the heat exchanger affected the outlet temperature. Figure 9 shows the different outlet temperatures corresponding to the length of the tubes with the two commonly used diameters of 0.05 m and 0.01 m and different tube numbers (10, 20, 30, 40, and 50). When the outlet temperature was decreased from 10 to 1°C, the tube length was increased twice.

For the same outlet temperature, as the number of tubes in the heat exchanger increases, the required length of the tubes becomes shorter, but the metal cost saved by the reduction in the tube length was far less than the increase in the number of tubes. For example, when the outlet temperature was set at 1°C and the tube diameter was 0.05 m, the number of tubes required was 10, 20, 30, 40, and 50, corresponding to tube lengths of 22.2 m, 19.3 m, 17.8 m, 16.7 m, and 16 m, respectively. The cost of a stainless steel pipe was $11.536 per meter; therefore, the corresponding costs were calculated as $2561, $4441, $6160, $7706, and $9229, respectively.

We also considered the heat dissipation of the fan during operation and the heat absorption during transportation. For the preliminary experiment in Shenyang, we selected a structure with 30 tubes that were 16 m in length with a tube diameter of 0.05 m.

3. Greenhouse cooling effect

Figure 10 shows that the greenhouse temperature was stable at a certain temperature when the greenhouse was closed at 12:25, and the temperature began to drop when the cooling system ran at 13:12. The cooling effect was best in the first end of bag air duct; the maximum cooling effect was 6.7°C, and the average cooling effect was 4.1°C. This was because the fluid velocity at the end of the pipe was small, increasing the heat exchange between the pipe and indoor air; therefore, the cooling effect was not obvious.

The best cooling effect of each group was at the measuring point of 2.5 m, with an average cooling effect of 4.8°C and maximum cooling effect of 6.7°C. The reason for the analysis is that the greenhouse air supply duct was arranged 3.5 m away from the greenhouse floor, and the measuring point of 2.5 m is the closest to the air supply duct; therefore, the measuring point of 2.5 m had the lowest temperature. The side wall of the air supply duct was inclined downward, and the density of the cold air is large and sinks; therefore, the measuring point of 4.5 m was the smallest. In summary, this cooling system had a certain effect in the cultivation area with a greenhouse length of less than 45 m.

4. Heat exchange pipe performance

Figure 11 shows the internal pipe temperature, heat transfer performance, and COP change inside the tubes. In the beginning, the temperature inside the tube drops rapidly, and then the temperature slows down later. The η and COP inside the heat exchange tubes increase as the length increases, and the rate gradually decreases. When the inlet temperature was 26°C, the maximum temperature difference between the inlet and outlet was 26°C, the maximum COP was 5.6, and the η was 100%. The η and COP of the exchange tubes were obviously reduced when the length of tubes was less than 8 m. Combined with the ice storage construction cost, it was more suitable to select 8 m for the heat exchange tube.

Table 4. Insulation material detailed parameters

	Density kg/m^3	Thermal conductivity W/(m·K)	Cost $
Block wall	2,150	0.24	Material and labor cost/m^3: 72.5 Material cost/m^3: 72.5
Expanded polystyrene	22	0.04	Installation cost/m^2: 29

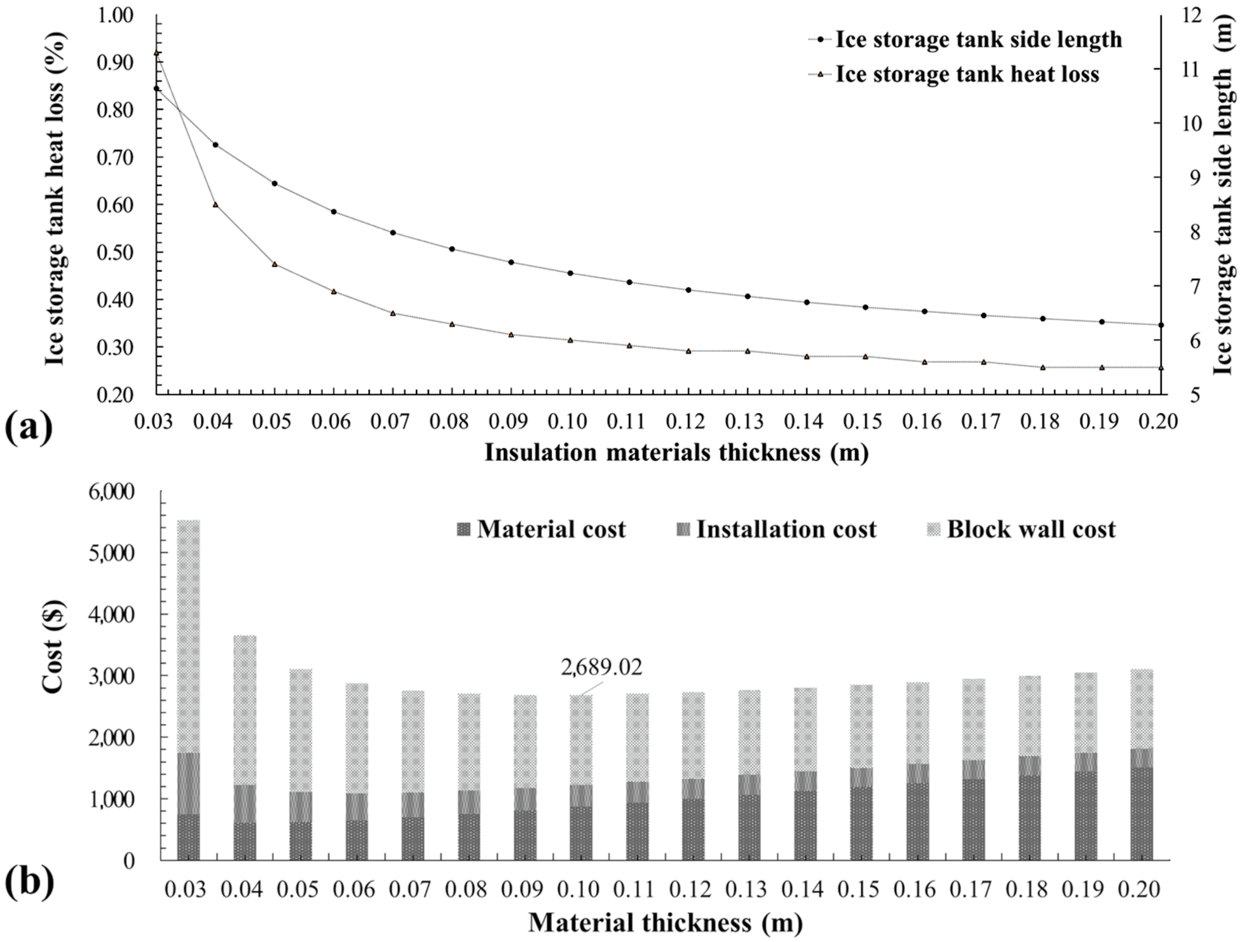

Fig. 8. (a) Relationships between insulation material thickness, storage tank heat loss, and tank side length; (b) ice storage tank cost for different thicknesses of insulation material

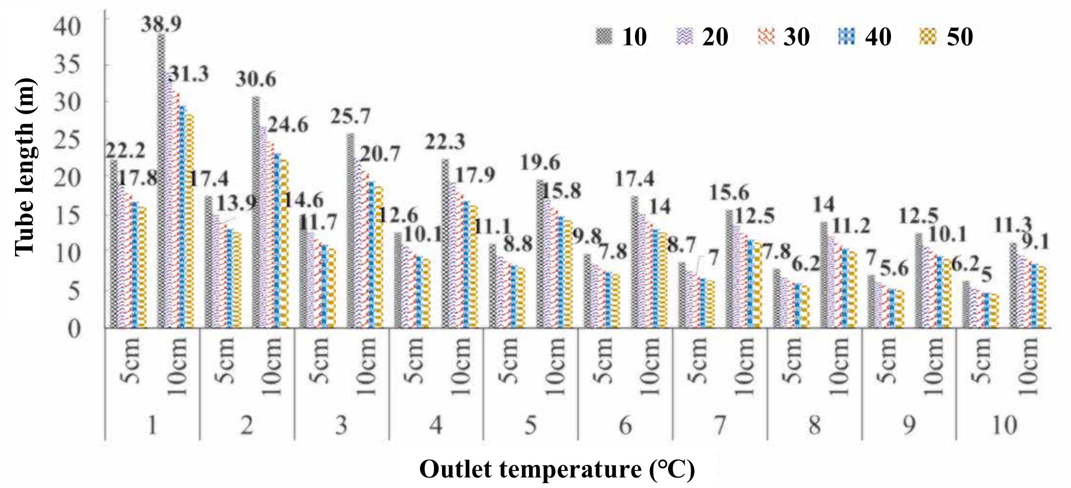

Fig. 9. Outlet temperature is directly related to the length of the pipe

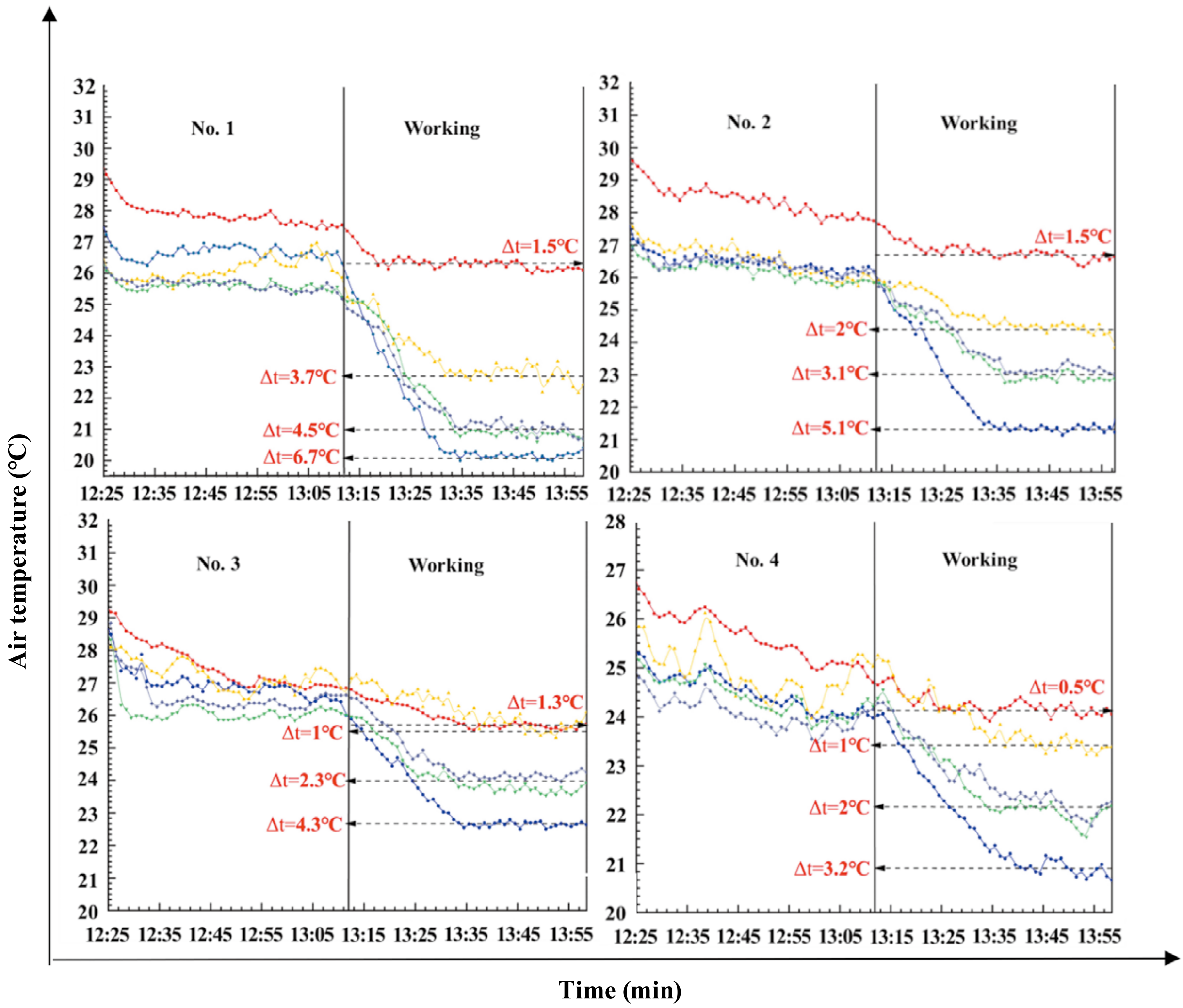

Fig. 10. Greenhouse measuring point cooling effect

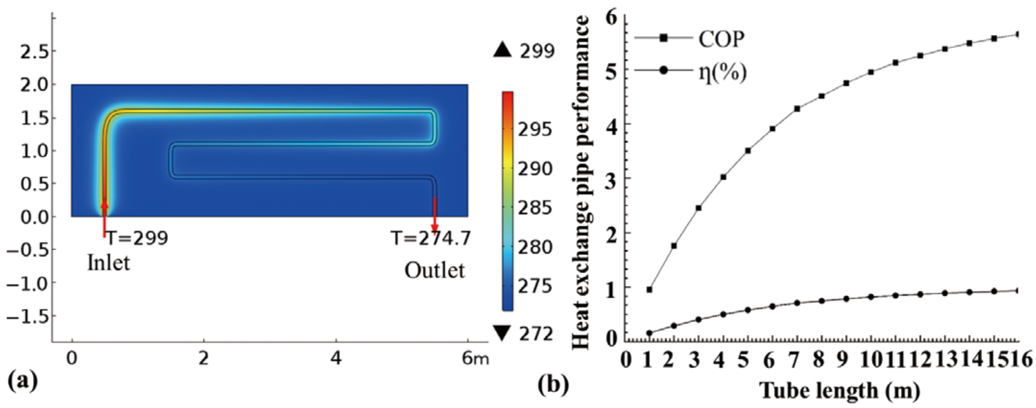

Fig. 11. (a) Simulation surface map (inlet: T = 299 K, V = 15.2 m/s); (b) changes in η and COP inside the tube vs. tube length

5. Ice storage cooling system performance

Using ice as a heat source for the heat exchanger can make the heat transfer performance of the heat exchange tube more stable because the ice water mixture is always at 0°C. Soil and water may increase the temperature along with the continuous absorption of air heat, which greatly affects the heat transfer performance.

Table 5 compares the performance of different heat exchange cooling systems: earth-to-air heat exchanger, water-to-air heat exchanger, and ice storage cooling. Using ice as a cold source, a higher temperature difference between the inlet and outlet can be obtained, obtaining more cooling capacity; this can also reduce the flow of the fan, reducing the power of the fan, achieving an energy-saving effect.

6. Application prospect

The ice storage cooling system is suitable for greenhouse cooling in areas with abundant natural cold sources. Considering the heat loss of the ice storage tank, the effective ice storage volume is 50.7 m^3, which can save 1.74×10^{10} J of power.

Combined with the initial construction of the system and the analysis of summer operation costs, the system is more suitable for use in greenhouses with better insulation and tightness in natural cold source areas. Greenhouses are suitable for summer high-quality or off-season vegetables and fruits, as well as the cultivation environment that requires low-light conditions for edible fungi.

Conclusions

In this study, we initially presented an energy-saving solution for the design of a practical cooling system for Chinese solar greenhouses. Using the seasonal ice storage system, cold energy can be stored in water in the winter and used as a cooling source to supply cold air in the summer. The parameters of the seasonal ice storage system were designed based on the cost of the materials and the cooling demands of the greenhouse during summer. We developed a CFD model and validated it for the selection of heat transfer pipes. Compared with other new energy-efficient cooling equipment, the proposed solution reduced the electricity consumption and increased the heat exchange performance to lower the air temperature. Additionally, our results will enable greenhouse architects and designers to develop more attractive and efficient designs for cooling in different areas around the world.

Table 5. Performance comparison of different heat exchange cooling systems

	Inlet and outlet temperature (°C)	Temperature difference (°C)	Cooling capacity (W)	Fan flow (m^3/h)	Greenhouse size (m^3)	Cooling effect (°C)	COP
Earth-to-air heat exchanger	32.5-28.5	4.0	243.5	208.8	45.0	1.0-3.7	1.9
Water-to-air heat exchanger	30.0-25.0	5.0	3,241.0	1,800.0	60.0	1.0-2.0	4.3
Ice storage cooling	26.0- 1.7	24.3	31,518.2	3,220.0	2,158.8	1.0-6.7	5.6

Table 6. Nomenclature and subscripts

A_{Ge}	greenhouse enclosure surface area (m^2)	T_{outd}	outdoor air temperature (°C)
A_n	each area of the ice storage pool (m^2)	T_{lim}	the max water thaw temperature (°C)
A_s	greenhouse floor area (m^2)	T_s	soil temperature (°C)
b	ice storage tank side length (m)	T_{ic}	soil temperature (°C)
C_a	specific heat capacity of air (J/kg·°C)	t_{in}	tube inlet temperature (°C)
C_{ic}	specific heat capacity of ice (J/kg·°C)	t_{out}	tube outlet temperature (°C)
C_{wa}	specific heat capacity of water (J/kg·°C)	Δt_{tw}	inside and outside the tube wall temperature difference (°C)
D	cooling days (d)	Δt_{loss}	temperature difference between the two sides of the ice storage tank enclosure (°C)

(Continued on next page)

Table 6. Nomenclature and subscripts (Continued)

D_1	inner diameter (m)	$\Delta t_{u\text{-}loss}$	temperature difference between ice storage tank and underground soil (°C)
D_2	external diameter (m)	$\Delta t_{t\text{-}loss}$	temperature difference between the top of the ice storage tank and the outdoor air (°C)
E	fan power (w)	u	tube flow rate (m/s)
G	the greenhouse cooling supply air rate (m^3/h)	v	the air speed property parameter (m^2/s)
Gr	Grashof number (dimensionless)	V_G	greenhouse volume (m^3)
h	convective heat transfer coefficient ($W/m^2 \cdot K$)	V_i	ice storage tank volume (m^3)
h_{fg}	ice melting heat (J/kg)	ρ	density (kg/m^3)
h_L	greenhouse indoor supply air enthalpy (KJ/kg)	ρ_a	air density (kg/m^3)
h_N	greenhouse indoor air enthalpy (KJ/kg)	ρ_{ic}	ice density (kg/m^3)
h_s	heat transfer coefficient from soil to greenhouse air ($W/m^2 \cdot K$)	ρ_{wa}	water density (kg/m^3)
k	heat transmition coefficient ($W/m^2 \cdot K$)	λ	thermal conductivity ($W/m \cdot K$)
k_{GE}	greenhouse enclosure heat transmition coefficient ($W/m^2 \cdot K$)	λ_a	air thermal conductivity ($W/m \cdot K$)
k_n	each area of the ice storage tank enclosed structure ($W/m^2 \cdot K$)	λ_b	brick walls thermal conductivity ($W/m \cdot K$)
k_{tu}	tube heat transmition coefficient ($W/m^2 \cdot K$)	λ_n	ice storage tank enclosure structure material thermal conductivity ($W/m \cdot K$)
L	length (m)	λ_{tu}	tube thermal conductivity ($W/m \cdot K$)
L_s	greenhouse floor length (m)	λ_{eps}	eps thermal conductivity ($W/m \cdot K$)
L_{tu}	tube length (m)	δ_b	brick walls thick (m)
m_a	air quality (kg)	δ_n	ice storage tank enclosure structure material thick (m)
n	the per unit time air changes (h)	η	heat exchange efficiency (%)
Nu	Nusselt number (dimensionless)	μ	dynamic viscosity ($N \cdot s/m^2$)
Pr	Prandtl number (dimensionless)	ω	ice storage tank heat loss rate (%)
q_c	greenhouse cooling load per unit time (J)	Φ	heat transfer tube total heat transfer quantity (W)
q_v	inlet air flow (m^3/s)	Subscripts	
Q_c	when the room temperature reaches set value, the greenhouse cooling load (J)	a	air
Q_{cool}	summer cold energy (J)	G	greenhouse
Q_f	before the room temperature reaches set value, the greenhouse cooling load (J)	Ge	greenhouse enclosure
Q_{loss}	the cooling loss during ice storage (J)	ic	ice
Q_h	heat exchange energy (J)	ind	indoor
Re	Reynolds number (dimensionless)	outd	outdoor
T_0	initial temperature of ice (°C)	s	soil
$T_{b\text{-}ind}$	cooling preconditioning period temperature (°C)	tu	tube
T_{ind}	indoor air temperature (°C)	wa	water

Acknowledgements

This research project was supported by the National Key Research Program of China (Grant No. 2016YFD0201004) and the China Agriculture Research System (Grant No. CARS-23-C01).

References

Álvarez-Prado, A. F. & Ploschuk, E. L. (2008) Development and growth of two *Lesquerella* species grown under different temperatures during the reproductive period. *Ind. Crops Prod.*, **27**, 400-403.

Blanchard, M. G. & Runkle, E. S. (2011) The influence of day and night temperature fluctuations on growth and flowering of annual bedding plants and greenhouse heating cost predictions. *HortScience*, **46**, 599-603.

Bordoloi, N. et al. (2018) An intense review on the latest advancements of Earth Air Heat Exchangers. *Renew. Sustain. Energy Rev.*, **89**, 261-280.

Catley, J. L. et al. (2002) Temperature and irradiance effects on *Sandersonia aurantiaca* flower shape and pedicel length. *Sci. Hortic.*, **93**, 157-166.

Chen, Y. Q. et al. (2014) Effect of difference between day and night temperature on fruit development and yield of tomato. *North Hortic.*, **24**, 38-42.

Cui, Y. et al. (2019) Techno-economic assessment of the horizontal geothermal heat pump systems: A comprehensive review. *Energ Convers. Manag.*, **191**, 208-236.

Davies, L. J. et al. (2002) Effects of day/night temperature differential and irradiance on the flower stem quality of *Sandersonia aurantiaca*. *Sci. Hortic.*, **95**, 85-98.

Erwin, J. E. et al. (2002) Interaction between photo period, GA3 and vernalization time on flowering of Raphanus sativus. *Physiol. Plant.*, **115**, 298-302.

Erwin, J. E. et al. (2002) Vernalization, photoperiod and GA3 interact to affect flowering of Japanese radish (Raphanus sativus Chinese Radish Jumbo Scarlet). *Physiol. Plant.*, **115**, 298-302.

Fang, G. (2006) *Energy storage air conditioning technology.* China Machine Press, Beijing, China.

Fleisher, H. D. et al. (2006) Effect of temperature perturbations on tomato (*Lycopersicon esculentum* Mill.) quality and production scheduling. *J. Hortic. Sci. Biotechnol.*, **81**, 125-131.

Francis, C. E. & Tamblyn, R. T. (1987) Annual cycle ice production and storage. *ASHRAE Trans.*, **93**, 1760-1765.

Ghani, S. et al. (2019) Design challenges of agricultural greenhouses in hot and arid environments: A review. *Eng. Agric. Environ. Food*, **12**, 48-70.

Ghosal, M. K. & Tiwari, G. N. (2006) Modeling and parametric studies for thermal performance of an earth to air heat exchanger integrated with a greenhouse. *Energy Convers. Manag.*, **47**, 1779-1798.

Hamada, Y. et al. (2007) Field measurements and analyses for a hybrid system for snow storage/melting and air conditioning by using renewable energy. *Appl. Energy*, **84**, 117-134.

Hamada, Y. et al. (2012) Study on a snow storage system in a renovated space. *Renew. Energy*, **41**, 401-406.

Hwang, S. J. et al. (2005) Effects of difference between day and night temperatures on growth and flowering of miniature roses. *Han'guk wŏnye hakhoe chi* (*J. Korean Soc. Hortic. Sci.*), **46**, 321-328 [In Korean with English summary].

Kim, S. H. et al. (2007) Growth and development of *Lilium longiflorum* 'Nellie White' during bulb production under controlled environments: I. Effects of constant, variable and greenhouse day/night temperature regimes on scale and stem bulblets. *Sci. Hortic.*, **112**, 89-94.

Kirkpatrick, D. L. et al. (1985) The ice pond—production and seasonal storage of ice for cooling. *Sol. Energy*, **35**, 435-445.

Kumar, K. S. et al. (2009) Design and technology for greenhouse cooling in tropical and subtropical regions: A review. *Energy Build.*, **41**, 1269-1275.

Kusakabe, M. (1962) Freezing degree days over Hokkaido. *Nihong sepyowu gakai* (*J. Japanese soc. Snow Ice*) (*Soppor Dist Meteorogical Observatory*), **24**, 185-188 [In Japanese with English summary].

Li, G. (2015) Research on seasonal ice cold energy storage technology for air conditioning cooling source. University of South China, Department of Civil Engineer, Hengyang, China.

Li, G. et al. (2015) Application of seasonal ice storage technology in stadium. *Low Temp. Archit. Technol.*, **37**, 48-51.

Li, L. et al. (2003) State and new technology on storage of fruits and vegetables in China. *Journal of Wuxi University of Light Industry* (*J. Wuxi Univ. Light Ind.*), **22**, 106-109 [In Chinese with English summary].

Li, L. (2007) *Study on the indoor thermal environment in a large space with cold air distribution system*. North China Electric Power University, Department of Engineering Thermophysics, Beijing, China.

Li, T. (2014) *Theory and practice on vegetable cultivation in solar greenhouse.* China Agriculture Press, Beijing, China.

Liu, X. & Guan, X. (2009) Seasonal snow cooling technology application in cold area airports. *Low Temp. Archit. Technol.*, **31**, 110-111.

López, A. et al. (2012) Sonic anemometry to evaluate airflow characteristics and temperature distribution in empty Mediterranean greenhouses equipped with pad–fan and fog systems. *Biosyst. Eng.*, **113**, 334-350.

Mao, L. et al. (2012) Effects of difference between day and night temperature on photosynthesis mechanism of tomato seedlings. *Acta Agric. Bor. Sin.*, **27**, 128-133.

Mongkon, S. et al. (2014) Cooling performance assessment of horizontal earth tube system and effect on planting in tropical greenhouse. *Energy Convers. Manag.*, **78**, 225-236.

Ni, L. et al. (2007) The history and future of aquifer thermal energy storage. *Build. Energy Environ.*, **26**, 18-24 [In Chinese with English summary].

Ou, Y. (2015) *Studies on the ice storage cold air distribution system*. Ji Mei University, Fujian, China [Thesis in Chinese with English summary].

Ozgener, L. & Ozgener, O. (2010) An experimental study of the exergetic performance of an underground air tunnel system for greenhouse cooling. *Renew. Energy*, **35**, 2804-2811.

Pakari, A. & Ghani, S. (2019) Evaluation of a novel greenhouse design for reduced cooling loads during the hot season in subtropical regions. *Sol. Energy*, **181**, 234-242.

Patil, G. G. & Moe, R. (2009) Involvement of phytochrome B in DIF mediated growth in cucumber. *Sci. Hortic.*, **122**, 164-170.

Perdigones, A. et al. (2008) Cooling strategies for greenhouses in summer: Control of fogging by pulse width modulation. *Biosyst. Eng.*, **99**, 573-586.

Sellami, D. et al. (2019) Comparative study of the performance of two greenhouse heating techniques: Solar air heater and heat pump. *Heat Transf. Res.*, **50**, 1127-1147.

Sethi, V. P. & Sharma, S. K. (2007) Greenhouse heating and cooling using aquifer water. *Energy*, **32**, 1414-1421.

Skogsberg, K. (2002) The Sundsvall Regional Hospital snow cooling plant—results from the first year of operation. *Cold Reg. Sci. Technol.*, **34**, 135-142.

Sun, W. et al. (2017) Nighttime cooling of solar greenhouse in summer based on water source heat pump system.

Res. Agric. Mod., **38**, 885-892 [In Chinese with English summary].
Verheul, M. J. et al. (2007) Influences of day and night temperatures on flowering of *Fragaria* x *ananassa* Duch., cvs. Korona and Elsanta, at different photoperiods. *Sci. Hortic.*, **112**, 200-206.
Vigneault, C. et al. (1990) Evaluation of stored winter coldness as a cooling source for precooling vegetables. *Canadian Agric. Eng.*, **32**, 285-289.
Wang, L. et al. (2007) Theoretical analysis of heat transfer law in a solidification process of ice-on-pipe. *J. Hebei Univ. Technol.*, **35**, 22-26 [In Chinese with English summary].
Warner, R. M. & Erwin, J. E. (2001) Variation in floral induction requirements of *Hibiscus* sp. *J Am. Soc. Hortic. Sci.*, **126**, 262-268.
Yan, C. et al. (2016a) A seasonal cold storage system based on separate type heat pipe for sustainable building cooling. *Renew. Energy*, **85**, 880-889.
Yan, C. et al. (2016b) Optimal design and application of a compound cold storage system combining seasonal ice storage and chilled water storage. *Appl. Energy*, **171**, 1-11.
Yang, S. & Tao, W. (2006) *Heat transfer.* Higher Education Press, Beijing, China, pp. 250-252.
Yang, Z. et al. (2014) Effect of difference between day and night temperature on nutrients and dry mass partitioning of tomato in climate chamber. *Nongye Gongcheng Xuebao* (*Transactions CSAE*), **30**, 138-147 [In Chinese with English summary].
Yıldız, A. et al. (2012) Energetic performance analysis of a solar photovoltaic cell (PV) assisted closed loop earth-to-air heat exchanger for solar greenhouse cooling: An experimental study for low energy architecture in Aegean Region. *Renew. Energy*, **44**, 281-287.
Yu, Y. et al. (2005) Present status and technology prospect of seasonal snow and ice storage. *HV&AC*, **35**, 24-30 [In Chinese with English summary].
Yu, Y. S. et al. (2010) Application of seasonal snow and ice thermal storage technology in building air conditioner. *Jiefangjun Ligong Da Xue Xuebao* (*J. PLA Univ. Sci. Technol.*), **11**, 339-343 [In Chinese with English summary].
Zhang, C. (2013) Thermal equilibrium analysis and verification of heat convection and radiation transfer in greenhouse at night. *J. Chn. Agric. Univ.*, **18**, 172-177.